High-pressure neutron diffraction study of $LaCoO_3$

Mara Capone, Christopher J Ridley, Nicholas P Funnell, Malcolm Guthrie and Craig L Bull

Published version information

This is the peer reviewed version of the following article:

Citation: M Capone et al. "High-pressure neutron diffraction study of $LaCoO_3$." Physica Status Solidi A, vol. 216, no. 6 (2019): 1800736.

DOI: 10.1002/pssa.201800736

HIGH-PRESSURE NEUTRON DIFFRACTION STUDY OF $LaCoO_3$

Mara Capone[1,2,3], Christopher J Ridley[1], Nicholas P Funnell[1], Malcolm Guthrie[2,3], Craig L Bull[*,1]

[1] ISIS Facility, Rutherford Appleton Laboratory, Chilton, Didcot OX11 0QX, UK
[2] European Spallation Source AB, PO Box 176, SE-22100, Lund, Sweden
[3] The School of Physics and the Centre for Science at Extreme Conditions, The University of Edinburgh, Peter Guthrie Tait Road, Edinburgh EH9 3FD, UK

Key words: High-pressure, perovskite, spin-state, structure

[*] Corresponding author: e-mail craig.bull@stfc.ac.uk

We report a high-pressure variable-temperature neutron diffraction study of $LaCoO_3$, from ambient to 6 GPa at 120, 290, and 480 K. We see no evidence for previously-reported discontinuities in the Co–O and La–O distances in the pressure and temperature ranges studied. Such discontinuities have previously been attributed to the well-documented spin-state transition of the Co^{3+} cation $\left(\text{from } t_{2g}^5 e_g^1, S=1 \rightarrow t_{2g}^6 e_g^0, S=0\right)$, we conclude that manifestations of the electronic configuration of $LaCoO_3$ are not evident in the crystallographic structure upon pressurisation. We also report bulk moduli for each of these temperatures as 134(2), 135(1), and 111(1) GPa respectively, as fitted to a second-order Birch-Murnaghan equation of state.

The electronic and magnetic properties of lanthanum cobaltate ($LaCoO_3$) has been a subject of interest for decades by virtue of its spin-state transitions[1–9]. $LaCoO_3$ is diamagnetic, and crystallises in the rhombohedral space group [4] $R\bar{3}c$(r) (see Figure 1) and undergoes well-characterised temperature-driven electronic transitions. At low temperature (< 50 K) $LaCoO_3$ is a non-magnetic insulator with trivalent cobalt in a low-spin-state configuration $t_{2g}^6 e_g^0$ ($S = 0$). At $\sim$100 K the material becomes paramagnetic and, with increasing temperature, a higher Co spin configuration is populated. There has been much interest as to whether the intermediate-spin $t_{2g}^5 e_g^1$ ($S = 1$) or the high-spin $t_{2g}^4 e_g^2$ ($S = 2$) state of the Co^{3+} is populated at this temperature [5,9–11]. Above 648 K charge transfer between Co cations is observed and disproportionation into Co^{2+} and Co^{4+} species occurs [12]. Such transitions are made possible by the small crystal field splitting of the Co d-orbitals; and thus thermal excitation of electrons from the t_{2g} state into the e_g state is readily achieved. Neutron diffraction has been extensively used to determine the crystal structure of $LaCoO_3$ with increasing temperature (from 4.2 – 1200 K) and, from an average structure perspective, the authors observed a linear increase in Co–O distance, with the CoO_6 polyhedra tending towards a 'cubic-like' octahedral geometry, and a decrease in the unit-cell angle (Figure 1) [4,13,5,14].

The spin-states of the Co cation in $LaCoO_3$ can also be altered by the application of high pressure as indicated by anomalies in magnetic measurements [15] and photoemission spectroscopy [16]. By X-ray diffraction Vogt *et al* [17] suggest that at $\sim$4 GPa there is a change in the compressibilities of the Co–O and La–O bonds. This was explained to be a result of pressure-induced depopulation of the intermediate spin-state between 0 – 4 GPa in favour of the low spin-state. Although this anomaly has been suggested to be a signature of the occurrence of such a transition, there is currently limited evidence to support this. A neutron diffraction study from 0 – 4 GPa, where only four pressures were measured, reports no unusual change in bond distances or structure with increasing pressure [18].

The La cations are surrounded by a 12-fold coordination shell of O anions (Figure 1) and there are three distinct La–O bonds: short (3 $\times$ La–O1), intermediate (6 $\times$ La–O2) and long (3 $\times$ La–O3). A temperature-dependent neutron diffraction study reported that the long La–O3 bond shows three anomalies at $\sim$100, 500, and 800 K, which have been attributed to spin-state transitions of the Co^{3+} cation, whereas no discontinuities were reported in the Co–O bond [5,13]. Furthermore, the pressure-dependent X-ray

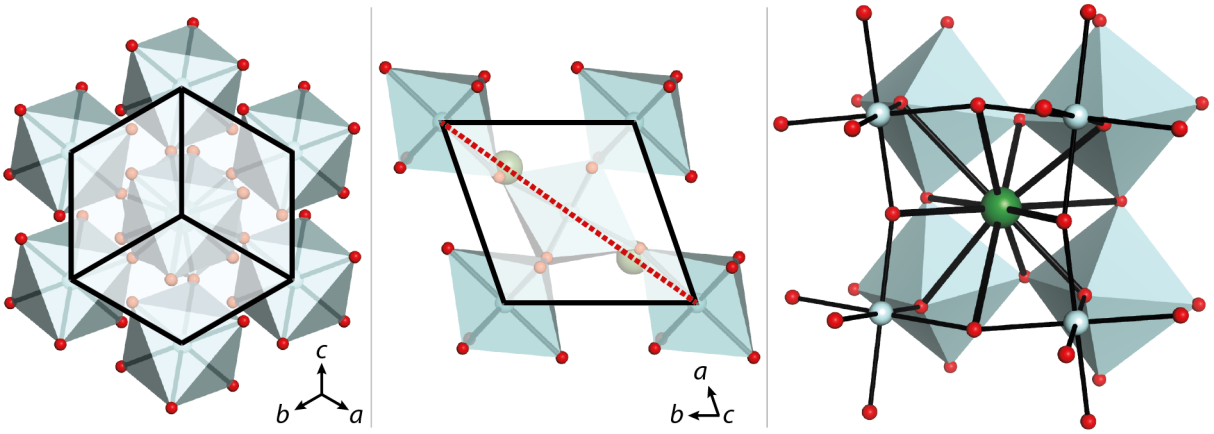

Figure 1 (Colour online) Crystal structure of $LaCoO_3$. Left panel: view down the <111> direction. The slightly opaque area shows the unit cell, and is outlined by the solid black line. La–O bonds are not shown for clarity. Middle panel: view along *c*-axis, the unit cell is again shown by solid black line and the angle subtended by the two lines is the unit-cell angle. Red dotted line indicates the <111> direction, as viewed in left panel, again, the La–O bonds are not shown for clarity. Right panel: picture showing the full bonding geometry of the La cation, which is surrounded by 12 oxygen atoms. In all panels the La, Co and O atoms are depiced as green, cyan and red spheres respectively.

diffraction study [17] also reports a discontinuity at 4 GPa on the La–O*i* ($i = 1, 2, 3$) bond lengths.

The lack of consensus in the literature on the structural changes of $LaCoO_3$ motivates our current high-pressure neutron diffraction study. We report structures to higher pressures than previously reported from neutron diffraction data [18]. Neutron diffraction is a more suitable tool for the accurate investigation of the structural parameters of transition-metal oxide systems due to the increased contrast between similar-*Z* atomic sites that cannot be achieved with X-ray diffraction. Precise measurements of the Co–O and La–O bond lengths are presented as a function of pressure at various temperatures. According to previous studies this information may be indicative of the nature of spin-state transitions in this compound.

$LaCoO_3$ was synthesised through nitrate decomposition as described elsewhere [13]. Neutron-powder diffraction measurements were performed at the temperatures of 120, 290, and 480 K in the 0 – 6 GPa pressure range on the PEARL instrument [19], at the ISIS neutron and muon facility, UK. Ground $LaCoO_3$ was loaded into an encapsulated null-scattering TiZr gasket. The sample volume also contained a small piece of lead, which acted as a pressure calibrant, and perdeuterated methanol:ethanol (4:1 by volume) was included to act as a hydrostatic pressure-transmitting fluid. The gasket was placed between a pair of single-toroidal anvils machined from zirconia-toughened alumina (ZTA) and force was applied to the anvil and gasket assembly by a modified V3 Paris-Edinburgh press which allows temperature control between 120 and 500 K [19]. Normalised neutron-diffraction patterns at 4 GPa at each measured temperature are shown in Figure 2. The data were Rietveld-refined using the GSAS suite of programmes [20] with $R\bar{3}c$ symmetry, in the rhombohedral cell-axis setting as reported previously for $LaCoO_3$ [4]. Experimental data showed that the rhombohedral crystal structure is preserved over the pressure ranges studied at each temperature. Refined structural parameters and details of the Rietveld fits as a function of pressure are reported in Tables S1, S2 and S3 (SI).

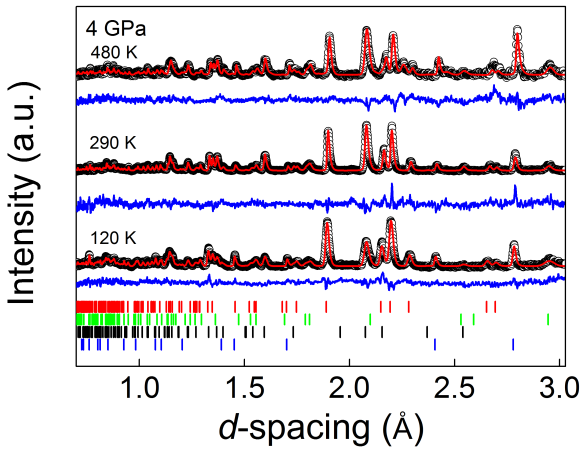

Figure 2 (Colour online) Neutron diffraction patterns of $LaCoO_3$ measured at $P \sim 4$ GPa, $T = 120$, 290 and 480 K. Open circles are the measured data, the red lines are the refined profiles, and the blue lines are the difference curves. The ticks represent (from top to bottom) positions of diffraction peaks of $LaCoO_3$, Al_2O_3 and ZrO_2 (from the anvils) and the pressure marker Pb, at 120 K.

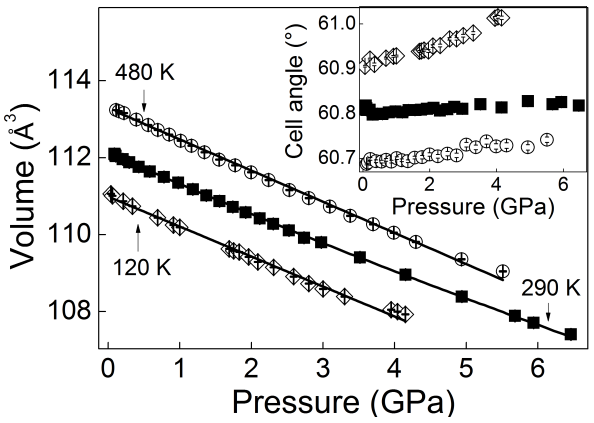

Figure 3 Pressure dependence of the unit cell volume at 120 K (open diamonds), 290 K (filled squares) and 480 K (open circles). Solid lines show fits to data with a second-order Birch-Murnaghan equation of state which yielded the B_0 and V_0 fitting values reported in Table 1. Inset shows the unit cell angle variation as a function of pressure. Error bars are shown but smaller than symbols.

The unit-cell volume evolution as a function of pressure is shown in Figure 3 at 120, 290, and 480 K. The bulk modulii (B_0) of the samples were determined by fitting a second-order Birch-Murnaghan equation of state (EoS) where the pressure derivative (B') was fixed at a value of 4. The values at each temperature are reported in Table 1. The determined ambient pressure unit cell volume $V_{0,290K}$ is comparable to literature values [13,4,5]. However, the values of B_0 are significantly lower than reported from previous studies 165(5) GPa [18], and 150(2) GPa [17], though slightly higher than 122(3) GPa reported by Zhou *et al* [21]. The large variation within these values may be a result of the limited number of pressure points collected in these studies. Similar to the finding from Zhou *et al* [21] the present study found that freely refining B' led to unphysical values. However, again we suggest that this may actually be due to an insufficient number of data points at higher pressures, and not a continuous spin-state transition.

The ambient pressure values of the rhombohedral angle (inset Figure 3) are in agreement with those previously reported for $LaCoO_3$ [13,4,5]. However, they display quite different behaviour upon compression at each temperature.

Table 1 Bulk modulus (B_0) and ambient pressure volume (V_0) determined with a second-order Birch-Murnaghan EoS at 120, 290 and 480 K. Also detailed are B_0 values previously reported in the literature.

T [K]	B_0 [GPa]	V_0 [Å^3]	$B_{0,\mathrm{lit}}$ [GPa]		
120	134(2)	111.01(2)	-	-	-
290	135(1)	112.12(1)	150(2)[17]	165(5)[18]	122(3)[21]
480	111(1)	113.38(1)	-	-	-

The rate of change in cell angle at ambient and high temperature upon compression is significantly lower than observed at low temperature. The compression of $LaCoO_3$ at 290 and 480 K is seen largely through reduction in the unit cell length, whereas at 120 K it is accommodated by both this and an increase in the rhombohedral angle.

Figure 4 (left) shows the variation in the determined Co–O bond distance as a function of pressure at each temperature. It was previously reported that the spin state transition in the Co^{3+} ion is manifested in the Co–O bond distance [17]. In our current study the Co–O bond lengths decrease linearly with increasing pressure at each temperature and no discontinuities are seen in the compressibilities. The value of the linear compressibility $k_{\mathrm{Co–O}}$ at 290 K (see Table 2) is the same within experimental error as the previously reported value of 0.0024(3) GPa^{-1} as determined by neutron diffraction [18], and the value reported for $La_{0.7}Sr_{0.3}CoO_3$, 0.0023 GPa^{-1}.[22] However, from the high pressure X-ray study reporting a discontinuity in the Co–O compressibility [17], the compressibilities $k_{\mathrm{Co–O}}$ before and after the spin-state transition were significantly different: 0.0045(2) and 0.0012(1) GPa^{-1}, respectively. Interestingly, in the current study the Co–O bond length compressibility remains unchanged at all temperatures investigated. If the evolution of the Co–O distance is indicative of the Co spin-state, then a larger difference in their compressibilities may be expected over the three temperatures measured [17]. Figure 4 (right) compares the Co–O bond length evolution at 290 K to previously reported neutron-diffraction [18] and X-ray values [17]. Although magnetisation [15], photoemission [16] and electrical measurements [23], show that this spin-state transition is promoted to higher temperatures by the application of pressure, no evidence for this was detected in the average Co–O bond length.

The compression of the La–O bonds from the present study is shown in Figure 5, no discontinuities have been observed over the pressure range studied at all temperatures. In contrast to that reported by Vogt *et al* [17] where the longest bond (La–O3) is seen to increase after the transition pressure of 4 GPa, we have found a linear decrease in the 0–6 GPa range, both for La–O3 and the intermediate bond La–O2. Their compressibilities are reported in Table 2. The pressure evolution of the shortest La–O1 bond length is reported in Table 2 as its variation is negligible in the pressure range studied and not shown in Figure 5. In the present study the compressibility of all bonds considered may be described by a simple linear relationship, rather than bilinear behaviour [17]. Full crystallographic data are reported in the SI. Differences between the present study and those reported elsewhere [17] may be a result of sample composition, however, the sample used in the present study has been previously characterised using high resolution neutron powder diffraction and the oxygen content has been refined to expected values [13]. The other possible difference is the presence of a $\sim$1% impurity of La_2O_3

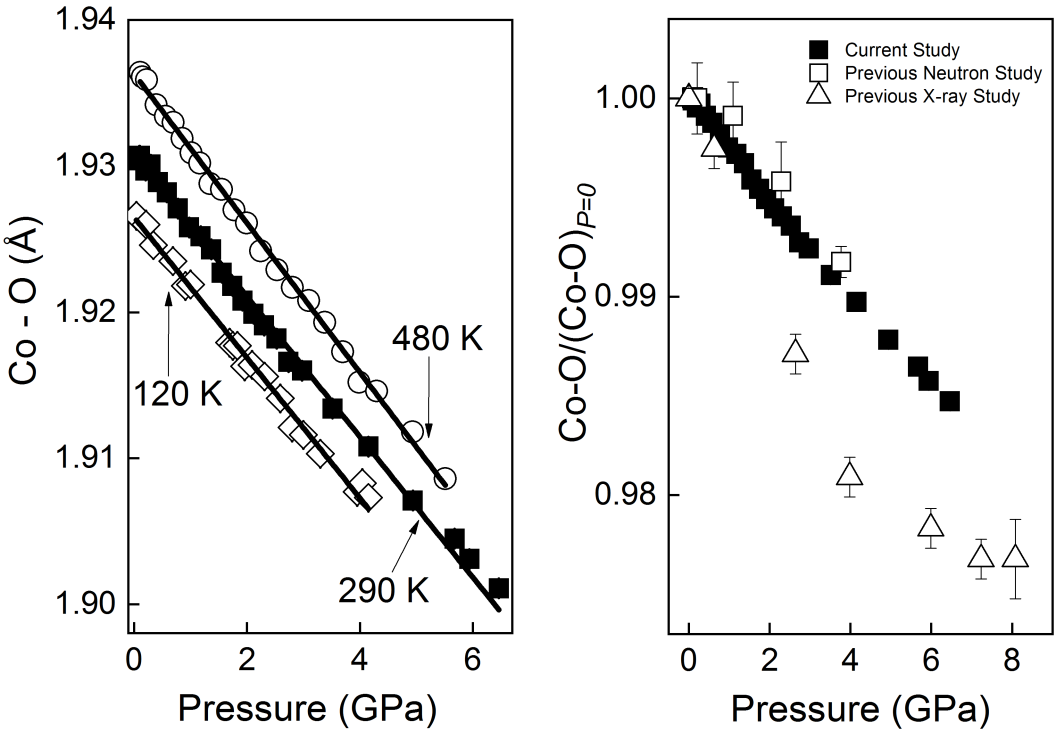

Figure 4 Left: Co–O bond lengths as a function of pressure at 120 K (open diamonds), 290 K (filled squares) and 480 K (open circles). Right: Relative change in Co–O bond distance with pressure at 290 K. Values for the present and previously reported studies [18,17] are shown for comparison. Error bars show determined uncertanties obtained from refinement (where not visible are smaller than symbols)

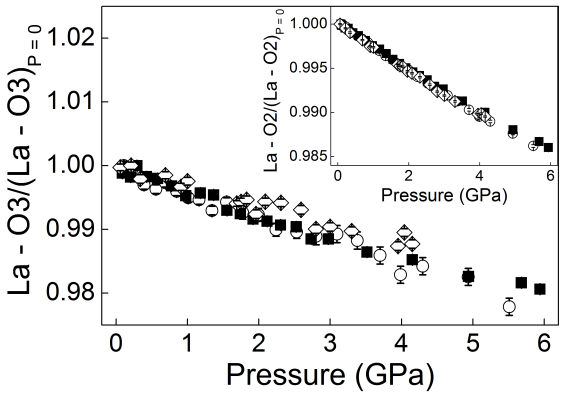

Figure 5 Variation in the La–O3 bond distance with pressure at 120 (open diamond), 290 (filled squares) and 480 K (open circles). Inset: pressure dependence of La–O2 bond distance. Error bars are also shown but smaller than symbols..

(fitted by Rietveld methods), however, at this level it is not expected to change the physical properties of $LaCoO_3$. However, the most likely cause for this discrepancy is the difference in techniques used in these studies, as discussed earlier.

In conclusion, a high-pressure study of $LaCoO_3$ has been reported in the 0–6 GPa range at 120, 290 and 480 K. The rhombohedral $R\bar{3}c$ crystal symmetry is maintained over this range. The change in unit cell volume has been investigated and the bulk modulus of $LaCoO_3$ has been determined at each temperature. Changes in the Co–O and La–Oi bond lengths have also been determined and a linear decrease has been reported over this range. The present neutron-diffraction study shows that changes to the well established electronic structure of $LaCoO_3$ are not manifested in the crystallographic structure.

Table 2 Compressibilities of Co–O and La–O bond distances for $LaCoO_3$ as $k = -L^{-1}_{P=0}\left(\frac{dL}{dP}\right)$. The final column shows the compressibilities determined from reference 17, showing one value for each pressure range 0–4/4–8 GPa where the discontinuity is observed.

k [GPa^{-1}]	120 K	290 K	480 K	$k_{290\,K}$ [17]
Co–O	0.0025(2)	0.0025(1)	0.0026(1)	0.0045(2)/0.0012(1)
La–O1	0.0012(2)	0.0008(1)	0.0006(2)	−0.013(3)/0.010(2)
La–O2	0.0026(1)	0.0024(1)	0.0026(1)	0.0027(2)
La–O3	0.0030(2)	0.0033(2)	0.0037(2)	0.018(3)/−0.006(2)

Acknowledgements We acknowledge Science and Technology Facilities Council (STFC) for providing the access to the PEARL instrument at the ISIS facility. We also acknowledge the European Spallation Source (ESS) and STFC as funding institutes of the studentship of M. Capone.

References

[1] K. Asai, P. Gehring, H. Chou, and G. Shirane, Phys. Rev. B **40**(Dec), 10982–10985 (1989).
[2] S. Yamaguchi, Y. Okimoto, and Y. Tokura, Phys. Rev. B **55**(Apr), R8666–R8669 (1997).
[3] C. Zobel, M. Kriener, D. Bruns, J. Baier, M. Grüninger, T. Lorenz, P. Reutler, and A. Revcolevschi, Phys. Rev. B **66**(Jun), 020402 (2002).
[4] G. Thornton, B. Tofield, and A. Hewat, Journal of Solid State Chemistry **61**(3), 301 – 307 (1986).
[5] P. G. Radaelli and S. W. Cheong, Phys. Rev. B **66**(Sep), 094408 (2002).
[6] K. Asai, A. Yoneda, O. Yokokura, J. M. Tranquada, G. Shirane, and K. Kohn, Journal of the Physical Society of Japan **67**(1), 290–296 (1998).
[7] J. Q. Yan, J. S. Zhou, and J. B. Goodenough, Phys. Rev. B **69**(Apr), 134409 (2004).
[8] H. Hsu, K. Umemoto, M. Cococcioni, and R. Wentzcovitch, Phys. Rev. B **79**(Mar), 125124 (2009).
[9] M. A. Korotin, S. Y. Ezhov, I. V. Solovyev, V. I. Anisimov, D. I. Khomskii, and G. A. Sawatzky, Phys. Rev. B **54**(Aug), 5309–5316 (1996).
[10] A. S. Panfilov, G. E. Grechnev, I. P. Zhuravleva, A. A. Lyogenkaya, V. A. Pashchenko, B. N. Savenko, D. Novoselov, D. Prabhakaran, and I. O. Troyanchuk, Low Temperature Physics **44**(4), 328–333 (2018).
[11] J. B. Goodenough, Journal of Physics and Chemistry of Solids **6**(2-3), 287–297 (1958).
[12] K. Knížek, Z. Jirák, J. Hejtmánek, P. Henry, and G. André, Journal of Applied Physics **103**(7), 07B703 (2008).
[13] C. L. Bull and K. S. Knight, Solid State Sciences **57**(C), 38–43 (2016).
[14] K. Knížek, P. Novák, and Z. Jirák, Phys. Rev. B **71**(Feb), 054420 (2005).
[15] K. Asai, O. Yokokura, M. Suzuki, T. Naka, T. Matsumoto, H. Takahashi, N. Mri, and K. Kohn, Journal of the Physical Society of Japan **66**(4), 967–970 (1997).
[16] G. Vankó, J. P. Rueff, A. Mattila, Z. Németh, and A. Shukla, Phys. Rev. B **73**(Jan), 024424 (2006).
[17] T. Vogt, J. A. Hriljac, N. C. Hyatt, and P. Woodward, Phys. Rev. B **67**(Apr), 140401 (2003).
[18] D. P. Kozlenko, N. O. Golosova, Z. Jirák, L. S. Dubrovinsky, B. N. Savenko, M. G. Tucker, Y. Le Godec, and V. P. Glazkov, Phys. Rev. B **75**(Feb), 064422 (2007).
[19] C. L. Bull, N. P. Funnell, M. G. Tucker, S. Hull, D. J. Francis, and W. G. Marshall, High Pressure Research **36**(4), 493–511 (2016).
[20] B. H. Toby, J. Appl. Crystallogr. **34**(2), 210–213 (2001).
[21] J. S. Zhou, J. Q. Yan, and J. B. Goodenough, Phys. Rev. B **71**(Jun), 220103 (2005).
[22] N. O. Golosova, D. P. Kozlenko, V. I. Voronin, V. P. Glazkov, and B. N. Savenko, Physics of the Solid State **48**(1), 96–101 (2006).
[23] R. Lengsdorf, M. Ait-Tahar, S. S. Saxena, M. Ellerby, D. I. Khomskii, H. Micklitz, T. Lorenz, and M. M. Abd-Elmeguid, Phys. Rev. B **69**(Apr), 140403 (2004).

Graphical Table of Contents

GTOC image:

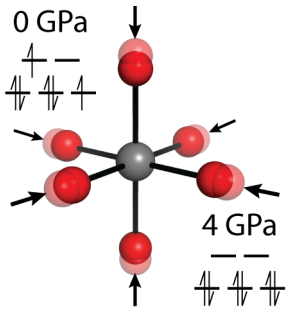

In a series of compressions to high-pressure (0–6 GPa) in the temperature-range 120–480 K we have used neutron diffraction to look for the manifestation of the well studied low-intermediate ($t_{2g}^6 e_g^0$ – $t_{2g}^5 e_g^1$) spin-state transition in $LaCoO_3$. In particular we have determined the compression behaviour of the Co–O bond within the CoO_6 octahrdra, previously suggested to be indicative of the electronic transitions.

Supplementary Information

Table S1 Structural parameters of $LaCoO_3$ as a function of pressure at 120 K, determined by Rietveld refinement. The atomic positions for La and Co cations in the proposed structure are: La ($\frac{1}{4},\frac{1}{4},\frac{1}{4}$) and Co (0,0,0), on the Wyckoff sites *2a* and *2b*, respectively. The oxygen atoms are located on the *6e* site (x ,$-$x + $\frac{1}{2},\frac{1}{4}$), hence, the O_x positions are the only refinable parameters in the Rietveld procedure as well as the unit cell parameters.. The R_p and R_{wp} values of the Rietveld fits are also reported.

P [GPa]	0.06(7)	0.21(7)	0.34(7)	0.69(7)	0.91(7)	1.00(7)	1.69(7)	1.75(7)
V [Å^3]	111.019(4)	110.871(5)	110.736(4)	110.444(4)	110.252(5)	110.188(5)	109.635(5)	109.577(4)
a [Å]	5.3584(1)	5.3555(1)	5.3538(2)	5.3485(2)	5.3453(2)	5.3442(2)	5.3348(1)	5.3339(2)
α [°]	60.907(2)	60.922(2)	60.910(3)	60.924(2)	60.928(2)	60.929(2)	60.939(2)	60.940(2)
O_x	0.1997(3)	0.1998(3)	0.2006(3)	0.1999(3)	0.2006(3)	0.2000(2)	0.2010(3)	0.2008(3)
Co–O [Å]	1.9300(2)	1.9260(3)	1.9246(2)	1.9235(2)	1.9218(2)	1.9219(2)	1.9179(2)	1.9177(3)
La–O1[Å]	2.442(2)	2.442(2)	2.446(2)	2.4399(16)	2.4423(17)	2.4387(18)	2.4404(13)	2.4388(18)
La–O2[Å]	2.6931(2)	2.6916(2)	2.6903(2)	2.6880(2)	2.6860(2)	2.6858(2)	2.68053(14)	2.6801(2)
La–O3[Å]	2.9893(16)	2.9877(17)	2.981(2)	2.9832(16)	2.9778(17)	2.980(2)	2.9701(13)	2.971(2)
R_{wp} [%]	6.20	6.46	7.88	6.11	6.40	7.38	4.71	6.53
R_p [%]	6.27	6.34	7.94	6.15	6.51	9.52	4.95	7.04
P [GPa]	1.83(7)	1.96(8)	2.09(8)	2.31(8)	2.59(8)	2.80(8)	3.00(8)	3.30(9)
V [Å^3]	109.546(5)	109.417(6)	109.288(5)	109.146(6)	108.908(6)	108.73(1)	108.59(1)	108.38(1)
a [Å]	5.3333(2)	5.3313(2)	5.3288(2)	5.3264(2)	5.3219(2)	5.3191(2)	5.3165(2)	5.3130(2)
α [°]	60.942(2)	60.940(3)	60.951(3)	60.952(3)	60.967(3)	60.967(3)	60.974(3)	60.980(3)
O_x	0.2006(3)	0.2015(3)	0.2004(3)	0.2002(3)	0.2004(4)	0.2017(4)	0.2014(4)	0.2015(4)
Co–O [Å]	1.9177(3)	1.9163(3)	1.9164(2)	1.9156(3)	1.9141(3)	1.9121(3)	1.9116(3)	1.9103(3)
La–O1[Å]	2.437(2)	2.441(2)	2.4344(17)	2.4326(18)	2.432(2)	2.437(2)	2.435(2)	2.434(2)
La–O2[Å]	2.6799(2)	2.6785(2)	2.67786(2)	2.6767(2)	2.6744(2)	2.6723(2)	2.6711(2)	2.6693(2)
La–O3[Å]	2.972(2)	2.965(2)	2.971(2)	2.970(2)	2.967(2)	2.958(2)	2.959(2)	2.957(2)
R_{wp} [%]	6.61	7.35	6.25	6.61	6.94	6.83	6.57	6.72
R_p [%]	6.87	7.85	6.44	6.90	6.83	6.81	6.51	6.73

P [GPa]	3.95(9)	4.04(9)	4.15(9)
V [Å^3]	108.04(1)	108.00(1)	107.93(1)
a [Å]	5.3061(3)	5.3053(2)	5.3042(3)
α [°]	61.013(4)	61.016(3)	61.014(4)
O_x	0.2024(4)	0.2011(3)	0.2019(4)
Co–O [Å]	1.9077(3)	1.9083(3)	1.9073(3)
La–O1[Å]	2.437(2)	2.430(2)	2.433(2)
La–O2[Å]	2.6654(2)	2.6656(2)	2.6647(2)
La–O3[Å]	2.950(2)	2.956(2)	2.951(2)
R_{wp} [%]	6.93	5.67	6.87
R_p [%]	7.02	5.49	6.90

Table S2 Structural parameters of $LaCoO_3$ as a function of pressure at 290 K, determined by Rietveld refinement. The atomic positions for La and Co cations in the proposed structure are: La ($\frac{1}{4},\frac{1}{4},\frac{1}{4}$) and Co (0,0,0), on the Wyckoff sites *2a* and *2b*, respectively. The oxygen atoms are located on the *6e* site (x ,$-$x + $\frac{1}{2},\frac{1}{4}$), hence, the O_x positions are the only refinable parameters in the Rietveld procedure as well as the unit cell parameters. The R_p and R_{wp} values of the Rietveld fits are also reported.

P [GPa]	0.09(7)	0.11(8)	0.09(6)	0.10(6)	0.20(6)	0.29(7)	0.43(6)	0.58(6)
V [Å^3]	112.100(4)	112.042(4)	112.086(3)	112.055(4)	111.957(3)	111.881(4)	111.764(3)	111.644(4)
a [Å]	5.3802(1)	5.3790(1)	5.3799(1)	5.3792(1)	5.3777(1)	5.3766(1)	5.3746(1)	5.3728(1)
α [°]	60.795(2)	60.801(2)	60.795(2)	60.803(2)	60.800(2)	60.798(2)	60.800(2)	60.799(2)
O_x	0.2030(3)	0.2024(3)	0.2028(3)	0.2029(3)	0.2031(3)	0.2020(3)	0.2028(2)	0.2027(3)
Co–O [Å]	1.9307(2)	1.9307(2)	1.9307(2)	1.9305(2)	1.9298(2)	1.9301(2)	1.9289(2)	1.9282(2)
La–O1[Å]	2.466(2)	2.463(2)	2.465(2)	2.466(2)	2.466(2)	2.459(2)	2.463(2)	2.461(2)
La–O2[Å]	2.7022(2)	2.7019(2)	2.7022(2)	2.7018(2)	2.7009(2)	2.7009(2)	2.6996(2)	2.69866(2)
La–O3[Å]	2.978(2)	2.981(2)	2.979(2)	2.978(2)	2.976(2)	2.982(2)	2.976(2)	2.976(2)
R_{wp} [%]	3.57	4.60	3.56	3.82	3.59	3.95	3.51	3.88
R_p [%]	3.82	5.27	3.62	4.08	3.46	4.13	3.38	4.20
P [GPa]	0.78(6)	0.97(2)	1.18(8)	1.37(7)	1.55(7)	1.74(7)	1.92(8)	2.12(8)
V [Å^3]	111.503(4)	111.345(4)	111.182(4)	111.019(4)	110.869(4)	110.718(4)	110.577(4)	110.418(4)
a [Å]	5.3703(1)	5.3677(1)	5.3652(1)	5.3623(1)	5.3599(1)	5.3574(1)	5.3551(1)	5.3525(1)
α [°]	60.803(2)	60.805(2)	60.803(2)	60.808(2)	60.808(2)	60.809(2)	60.811(2)	60.813(2)
O_x	0.2032(3)	0.2037(3)	0.2032(3)	0.2031(3)	0.2042(3)	0.2043(3)	0.2045(3)	0.2044(3)
Co–O [Å]	1.9271(2)	1.9258(2)	1.9252(2)	1.9243(2)	1.9227(2)	1.9218(2)	1.9208(2)	1.9199(2)
La–O1[Å]	2.463(2)	2.465(2)	2.461(2)	2.459(2)	2.464(2)	2.463(2)	2.464(2)	2.462(2)
La–O2[Å]	2.6972(2)	2.6956(2)	2.6946(2)	2.6932(2)	2.6914(2)	2.6902(2)	2.6889(2)	2.6876(2)
La–O3[Å]	2.972(2)	2.967(2)	2.969(2)	2.968(2)	2.9610(2)	2.959(2)	2.957(2)	2.956(2)
R_{wp} [%]	4.03	4.13	4.19	4.21	4.28	4.28	4.38	4.38
R_p [%]	4.58	4.66	4.97	4.69	4.89	5.04	5.81	5.10
P [GPa]	2.30(8)	2.52(8)	2.73(8)	2.98(7)	3.52(8)	4.15(1)	4.93(1)	5.67(1)
V [Å^3]	110.276(4)	110.114(4)	109.925(5)	109.799(5)	109.407(5)	108.964(5)	108.385(6)	107.892(6)
a [Å]	5.3504(1)	5.3476(1)	5.3444(1)	5.3425(1)	5.3357(1)	5.3288(1)	5.3188(2)	5.3110(2)
α [°]	60.807(2)	60.810(2)	60.815(2)	60.811(2)	60.821(2)	60.814(2)	60.828(3)	60.821(3)
O_x	0.2045(3)	0.2044(3)	0.2052(3)	0.2049(3)	0.2055(3)	0.2054(3)	0.2059(4)	0.2055(4)
Co–O [Å]	1.9191(2)	1.9182(2)	1.9166(2)	1.9160(2)	1.9134(2)	1.9108(2)	1.9071(3)	1.9045(3)
La–O1[Å]	2.462(2)	2.460(2)	2.463(2)	2.460(2)	2.460(2)	2.456(2)	2.455(2)	2.449(2)
La–O2[Å]	2.6865(2)	2.6859(2)	2.6839(2)	2.6824(2)	2.67870(18)	2.6753(2)	2.6699(2)	2.6663(2)
La–O3[Å]	2.954(2)	2.953(2)	2.947(2)	2.947(2)	2.941(2)	2.938(2)	2.930(2)	2.928(2)
R_{wp} [%]	4.38	4.30	4.35	4.33	4.25	4.36	5.25	5.17
R_p [%]	5.30	5.15	5.16	5.00	4.91	5.06	6.93	6.85
P [GPa]	5.93(1)	6.46(1)						
V [Å^3]	107.713(6)	107.414(6)						
a [Å]	5.3079(2)	5.3032(2)						
α [°]	60.826(3)	60.818(3)						
O_x	0.2059(4)	0.2063(4)						
Co–O [Å]	1.9032(3)	1.9011(3)						
La–O1[Å]	2.450(2)	2.449(2)						
La–O2[Å]	2.6645(2)	2.6620(2)						
La–O3[Å]	2.924(2)	2.919(2)						
R_{wp} [%]	5.49	5.29						
R_p [%]	7.06	6.88						

Table S3 Structural parameters of $LaCoO_3$ as a function of pressure at 480 K, determined by Rietveld refinement. The atomic positions for La and Co cations in the proposed structure are: La ($\frac{1}{4},\frac{1}{4},\frac{1}{4}$) and Co (0,0,0), on the Wyckoff sites *2a* and *2b*, respectively. The oxygen atoms are located on the *6e* site (x ,$-$x + $\frac{1}{2},\frac{1}{4}$), hence, the O_x positions are the only refinable parameters in the Rietveld procedure as well as the unit cell parameters. The R_p and R_{wp} values of the Rietveld fits are also reported.

P [GPa]	0.11(2)	0.15(2)	0.22(2)	0.39(2)	0.56(2)	0.69(2)	0.85(2)	1.01(2)
V [Å^3]	113.236(5)	113.209(6)	113.163(6)	112.991(6)	112.854(6)	112.717(6)	112.605(7)	112.436(7)
a [Å]	5.4026(2)	5.4020(1)	5.4010(2)	5.3985(2)	5.3963(2)	5.3939(2)	5.3923(2)	5.3893(2)
α [°]	60.688(2)	60.691(3)	60.699(3)	60.694(3)	60.693(3)	60.697(3)	60.693(3)	60.701(3)
Ox	0.2031(4)	0.2041(4)	0.2041(4)	0.2051(4)	0.2051(4)	0.2046(4)	0.2051(5)	0.2053(5)
Co–O [Å]	1.9364(3)	1.9361(3)	1.9359(3)	1.9342(3)	1.9334(3)	1.9330(3)	1.9319(3)	1.9309(3)
La–O1	2.478(2)	2.479(2)	2.479(2)	2.483(2)	2.482(2)	2.478(2)	2.480(3)	2.480(3)
La–O2	2.7130(2)	2.7126(2)	2.7121(2)	2.7103(2)	2.7092(2)	2.7083(2)	2.7072(3)	2.7056(3)
La–O3	2.981(2)	2.980(2)	2.979(2)	2.972(2)	2.971(2)	2.973(2)	2.969(3)	2.966(3)
R_{wp} [%]	3.84	4.11	4.15	4.05	4.31	4.35	4.55	4.57
R_p [%]	4.10	4.61	4.54	4.41	4.65	4.49	4.87	4.89
P [GPa]	1.16(2)	1.34(2)	1.55(2)	1.77(2)	1.99(3)	2.24(3)	2.53(2)	3.01(3)
V [Å^3]	112.307(7)	112.144(7)	111.952(8)	111.799(8)	111.623(8)	111.415(9)	111.16(1)	110.95(1)
a [Å]	5.3874(2)	5.3849(3)	5.3815(3)	5.3790(3)	5.3759(3)	5.3728(2)	5.3685(4)	5.3652(4)
α [°]	60.696(3)	60.694(3)	60.702(3)	60.703(4)	60.709(4)	60.705(4)	60.711(5)	60.707(5)
O_x	0.2053(5)	0.2059(5)	0.2049(5)	0.2057(5)	0.2055(6)	0.2066(6)	0.2063(6)	0.2063(7)
Co–O [Å]	1.9302(3)	1.9288(4)	1.9284(4)	1.9270(4)	1.9261(4)	1.9242(4)	1.9229(4)	1.9217(5)
La–O1	2.479(3)	2.481(3)	2.474(3)	2.477(3)	2.475(3)	2.479(3)	2.476(3)	2.475(4)
La–O2	2.7047(3)	2.7031(3)	2.7019(3)	2.7003(3)	2.6988(3)	2.6967(3)	2.6947(3)	2.6930(4)
La–O3	2.965(3)	2.960(3)	2.964(3)	2.959(3)	2.958(3)	2.951(3)	2.950(3)	2.948(4)
R_{wp} [%]	4.52	4.59	4.61	4.74	4.65	4.68	4.64	4.69
R_p [%]	4.88	4.80	4.91	5.03	5.00	4.98	5.09	5.18

P [GPa]	3.09(2)	3.38(3)	3.70(3)	3.99(2)	4.30(2)	4.93(2)	5.51(2)
V [Å^3]	110.73(1)	110.49(1)	110.26(1)	110.04(1)	109.81(1)	109.35(1)	109.05(1)
a [Å]	5.3607(4)	5.3572(4)	5.3530(4)	5.3498(4)	5.3459(4)	5.3387(5)	5.3330(5)
α [°]	60.731(5)	60.725(5)	60.738(6)	60.727(6)	60.729(6)	60.725(6)	60.742(6)
O_x	0.2058(7)	0.2060(7)	0.2070(7)	0.2082(8)	0.2071(8)	0.2073(8)	0.2094(8)
Co–O [Å]	1.9208(5)	1.9193(5)	1.9173(5)	1.9152(5)	1.9146(5)	1.9118(5)	1.9086(5)
La–O1	2.470(4)	2.470(4)	2.473(4)	2.478(4)	2.471(4)	2.468(4)	2.478(5)
La–O2	2.6910(4)	2.6892(4)	2.6866(4)	2.6845(4)	2.6830(4)	2.6793(4)	2.6755(4)
La–O3	2.949(4)	2.946(4)	2.939(4)	2.930(4)	2.934(4)	2.929(4)	2.915(5)
R_{wp} [%]	4.91	4.89	4.91	4.92	4.93	4.93	4.61
R_p [%]	5.27	5.40	5.30	5.22	5.36	5.27	4.28